Hypersonic Lee Surface Flow Phenomena over a Space Shuttle

V. Zakkay,* M. Miyazawa,† and C.R. Wang‡
New York University, Westbury, N.Y.

Leeward surface pressure and heat-transfer, flow separation, flowfield, and oil flow patterns of a space shuttle model are investigated experimentally at $0° \leq \alpha \leq 40°$ and a freestream Mach number of 6. The freestream Reynolds numbers were varied between 1.64×10^7 and 1.31×10^8 with different stagnation pressures. Results of experiment indicate two distinct types of flow separation and surface heating, depending on the angle of attack. Large axial components of velocity are also calculated in the separated flow region. Turbulent boundary-layer theory with a separation shape factor of 1.9 agrees with the heat-transfer measurements for $\alpha > 0°$. Inviscid supersonic flow theory over an equivalent body geometry also agrees approximately with the profile measurements of the flowfield on the leeward plane of symmetry.

Nomenclature

C_P	= pressure coefficient
L	= body length of the model
M	= Mach number
P	= pressure
q	= heat-transfer rate
R_∞	= freestream unit Reynolds number per meter
$R_{\infty L}$	= freestream Reynolds number based on model length
T	= temperature
V	= flow velocity
$X, Y, Z,$	= body axes
α	= angle of attack
θ_c	= cone half-angle

Subscripts

P	= conditions at peak heating
s	= separation
t	= total stagnation conditions
t_2	= local stagnation conditions behind a normal shock
w	= conditions at the wall
w_0	= laminar stagnation conditions
∞	= freestream conditions
0∞	= freestream stagnation conditions

I. Introduction

A complete description of the leeward surface heating of a space shuttle orbiter requires an understanding of 3-dimensional flow separation, vortices lifting off the surface, and effect of the freestream conditions on the flowfield. Initial research on lee-surface heating and flow separation over delta wing and several conceptual space shuttles has been done.[1-6] Effects of the freestream Mach number, Reynolds number, and angle of attack were also discussed. Results of this previous work have shown that coiled-vortex sheets on the lee surface induce a downward flow of high energy air toward the centerline, which then turns outward, drawing low energy fluid from the center area. Two heating peaks, due to the existence of vortex system and boundary-layer transition of the reattachment flow, also were found. Wang[7] has shown that, for a spheriod with moderate thickness ratio, a bubble-type separation prevails at low incidence, a free-vortex-type separation dominates at high incidence, and the separation reverts to a closed-bubble-type as the incidence continues to increase. Maskell[8] studied the 3-dimensional flow separation without using the boundary-layer concept. He has shown that: a) Three dimensional separated flow consists of two basic types: a bubble type and a free-vortex type, each of which is characterized by a particular form of surface flow pattern. b) The bubble-type separation requires the existence of a singular point. c) Separation line for a free-vortex layer has only regular points. d) A combination of these two types of flow patterns is the general result of flow separation. e) The flow separation can be inferred from a study of the surface flow pattern if it does indicate the nature of limiting streamlines.

Because there is a sparsity of experimental surface and flowfield data for similar flow conditions on the space shuttle and there is concern for the surface heating on the leeward side, further research is required to verify the possibility of using existing flowfield results over similar body geometries to analyze space shuttle flow phenomena. In the present investigation, theory and experiment have been undertaken to examine the following problems: a) The surface heat transfer on the leeward side of the space shuttle with different freestream Reynolds numbers and angles of attack. b) The peak heating due to boundary-layer transition and flow separation and comparison of the correlation of surface peak heating over different space shuttle configurations. c) The leeward flowfield in the vortex flow region and the method of constructing an equivalent model for leeward flowfield analysis.

II. Experiment

Present experiments were performed in a Mach 6 blowdown-type axisymmetric wind tunnel. The test section of the tunnel is 30.5 cm in diameter. For all the tests of present experiments, stagnation temperatures were nominally 500 K and the stagnation pressure is varied from 1.38×10^6 to 1.38×10^7 N/m^2. The resulting freestream Reynolds numbers were in the range of 1.64×10^7 to 1.31×10^8 /m.

Models

Based on an early NASA shuttle design, two space shuttle models with identical configurations were used in the tests. The model used for surface heat-transfer measurements was instrumented with chromel-alumel thermocouples welded to the inside surface of the model. Thickness of the wall (stainless steel) on the nose part varies from 0.053 cm - 0.081 cm. Stainless-steel shimstock of 0.025-cm thickness, was used

Presented as Paper 75-148 at the AIAA 13th Aerospace Sciences Meeting, Pasadena, California, January 20-22, 1975; submitted January 31, 1975; revision received May 27, 1975. This work was supported by NASA under Grant NGR-33-016-179.

Index categories: Boundary Layers and Convective Heat Transfer-Laminar; Boundary-Layer Stability and Transition.

*Professor of Applied Science. Associate Fellow AIAA.

†Formerly Assistant Research Scientist.

‡Associate Research Scientist.

for the other parts of the model. The other model, used for surface pressure measurements, was equipped with pressure taps having 0.16-cm orifice diameters. Scanivalves and transducers, calibrated for very small pressure range, were used to sense pressure through the orifice. Pressure and temperature data were recorded on a multichannel visicorder through galvanometers with response time less than 0.01 sec.

A special support for the space shuttle model was constructed. It consists of two semicircular struts. The struts were attached to the wing tips to avoid interactions which would affect the base pressure, and the leeward flowfield. All leads of thermocouples and pressure taps were taken through a groove inside the strut.

Surface Heat-Transfer and Pressure Measurements

The transient thin-wall technique was used to calculate the local heat-transfer rate from the slope of the temperature-time record. In this technique, a sharp slope at zero time is necessary. For this purpose the whole nozzle section was evacuated well below the expected freestream static pressures before each test and the flow became steady within a half second after the tests started. Heat-transfer data obtained were reduced to a dimensionless form q_w/q_{w0}, with q_{w0} being the stagnation heat-transfer rate on a sphere of 0.38-cm radius calculated from Lees' theory.[9] Local surface pressure measured over the space shuttle model was normalized with respect to the freestream static pressure.

Surface Heat-Transfer and Pressure Measurements

The transient thin-wall technique was used to calculate the local heat-transfer rate from the slope of the temperature-time record. In this technique, a sharp slope at zero time is necessray. For this purpose the whole nozzle section was evacuated well below the expected freestream static pressure before each test and the flow became steady within a half second after the tests started. Heat-transfer data obtained were reduced to a dimensionless form q_w/q_{w0}, with q_{w0} being the stagnation heat-transfer rate on a sphere of 0.38-cm radius calculated from Lees' theory.[9] Local surface pressure measured over the space shuttle model was normalized with respect to the freestream static pressure.

Flowfield Surveys

Total pressure, static pressure, and total temperature along the leeward plane of symmetry were measured with three different boundary-layer probes. These measurements were performed by traversing the probes perpendicularly to the body axis. To minimize the error introduced by the shock boundary-layer interaction due to the presence of the probe in the supersonic region, streamline shaped probes were used. The static probe has a conical tip faired into a 0.10-cm hypodermic needle. Lateral orifices located 10-15 probe diameters downstream were drilled in the probe. The total pressure probe consists of a hypodermic needle having a diameter of 0.1 cm flattened at the tip with a thickness of 0.015 cm and an opening of 0.005 cm. The total temperature probe was made of an unshielded, open-tip chromel-alumel thermocouple.

Oil Flow Studies

Oil flow techniques were employed to determine the surface (limiting) streamlines, and separation patterns on the surface of the space shuttle. Before each test, a mixture of Dow Corning 200 silicone oil (50-100 centistokes) and carbon black powder was sprayed over the entire model surface. In the oil flow studies, Dow Corning silicone oil with the viscosity between 70 and 100 centistokes was found to produce the best results when properly mixed with black carbon.

Table 1 Test conditions

Measurements	α(deg)	$R_{\infty,L} \times 10^7$
Surface heat transfer	0→40	0.32→2.57
Surface pressure	0→40	0.5 →2.42
Flowfield survey	20→30	0.61→2.31
Oil flow	10→40	0.92→2.39

III. Results and Discussions of Experiment

Details of the experimental data can be found in Ref. 10. However, the test conditions are shown in Table 1, with

$$M_\infty = 5.93$$
$$P_{0\infty} = 1.38 \times 10^6 - 1.38 \times 10^7 \text{N/m}^2$$
$$T_{0\infty} = 450 - 500 \text{ K}$$
$$T_w/T_{0\infty} = 0.6 - 0.7$$

Distribution of Surface Pressure and Heat-Transfer Rate on Lee Surface

Examples of surface pressure distribution for $\alpha = 0°$ and 30° along the leeward centerline are given in Fig. 1. At zero angle of attack, the surface pressure distribution is slightly influenced by the changes in the freestream Reynolds number. For comparison, surface pressure on a sharp cone[11] having the same cone half-angle, $\alpha = 19.3°$ is also shown in the figure. The cone values agree with present experimental results over the nose region of the model at high Reynolds number. As the angle of attack increases, Reynolds number affects the surface pressure in the region after the expansion corner; lower pressure level is found with a higher freestream Reynolds number. Thus, the viscous interaction is significant in this region. Similar results have been found in Ref. 12. The strongest viscous interaction effect is found at $\alpha = 30°$ in the present experiments, particularly in the region after the expansion corner.

All the heat-transfer data presented here were nondimensionalized by the theoretical laminar stagnation point heat-transfer rate, q_{w0}, on a sphere ($r = 0.38$ cm) having the same nose radius as the model at the same test conditions. In the present investigation, the theoretical value obtained from Lee's method was used.

To assess the results of the heat-transfer data and compare them with a reference point, some estimates have been made based on the measured surface pressure distribution and 2-dimensional or axisymmetric boundary-layer assumptions neglecting the cross-flow effects. Two extreme entropy relations were used to determine the local external flow conditions; conditions were assumed based on a normal shock, conical shock due to a sharp cone, $\theta_c = 19.3°$, at zero angle of attack. The modified Lees method[13] was used for laminar calculation. Turbulent heat-transfer rates were calculated by the Reshotko-Tucker method,[14] and the Flat Plate Reference Enthalpy Method.[15] Estimates were based on the measured surface pressure distributions corresponding to each heat-transfer test and the assumption that attached boundary-layer flow exists on the lee surface. Results are compared with experimental measurements in Figs. 2-4.

The effect of Reynolds number on lee-surface heat-transfer rates at a specified angle of attack are also shown in Figs. 2-4. Separation points determined from oil flow studies are shown for cases with $\alpha > 0°$.

At $\alpha = 0°$ (Fig. 2) a comparison of the data with theory indicates that a laminar boundary-layer flow exists over the major portion of the lee surface. Although the space shuttle orbiter is a 3-dimensional body and the laminar estimate[13] assumes a highly cooled wall with the negligible effect of local pressure gradient, the laminar axisymmetric calculation agrees reasonably well with measurements in the front portion before the shoulder. After the shoulder, scattering experimental data are found.

At $\alpha = 10°$, the maximum heat-transfer rate in the nose region is approximately equal to that for a 2-dimensional turbulent boundary layer for the case of $R_{\infty,L} = 2.42 \times 10^7$. For other $\alpha = 10°$ cases, experiments are in good agreement with laminar boundary-layer theory. Boundary-layer transition occurs in the nose region as the freestream Reynolds number in-

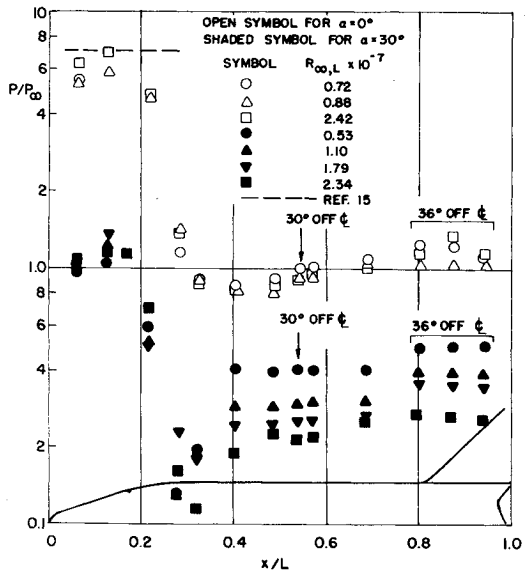

Fig. 1 Surface pressure distributions along leeward centerline.

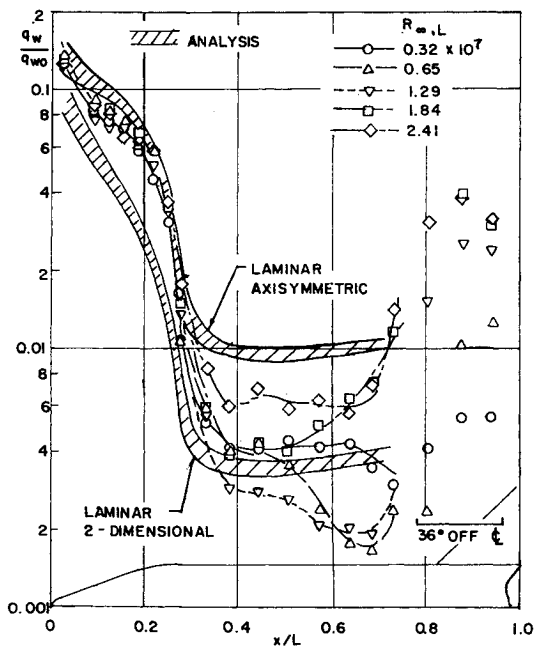

Fig. 2 Heat-transfer distributions along leeward centerline ($\alpha = 0°$).

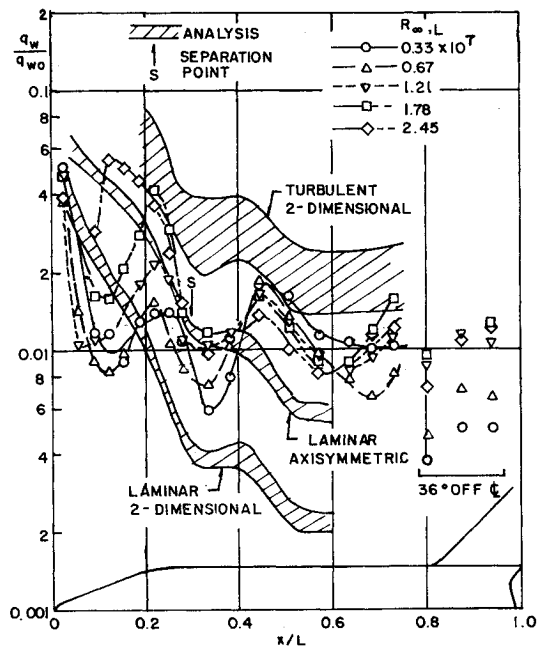

Fig. 3 Heat-transfer distributions along leeward centerline ($\alpha = 20°$).

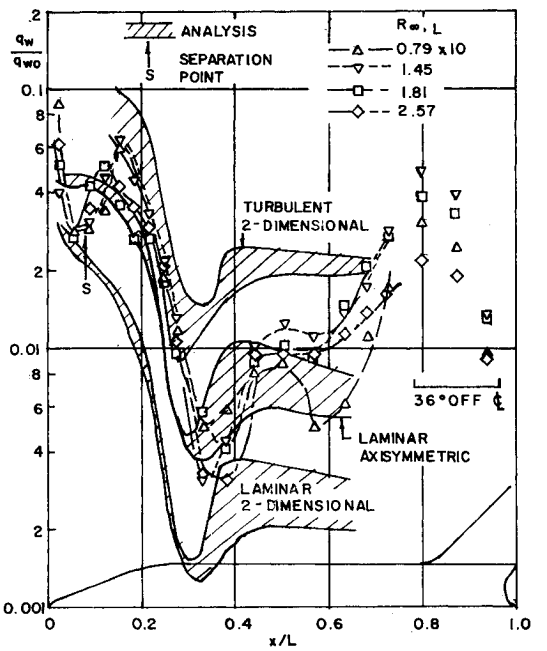

Fig. 4 Heat-transfer distributions along leeward centerline ($\alpha = 30°$).

creases. This tendency becomes more evident at an angle of attack of 20° (Fig. 3) where turbulent boundary layer is believed to exist over the nose portion at $R_{\infty,L} = 2.42 \times 10^7$. Peak heating also appears in the nose region for $\alpha = 10°$ and 20°. This suggested that peak heating is due to boundary-layer transition for the case of small angle of attack. At $\alpha = 20°$, another peak heating appears in the region after the expansion shoulder. This is due to the flow separation, and will be discussed later.

For high angles of attack ($\alpha = 30°$, 40°), peak heating phenomena associated with flow separation, termed the vortex-induced peak heating, are observed (Fig. 4). In both cases, the maximum heating values are found to be nearly the same order of magnitude as the local turbulent heat-transfer rates calculated from attached boundary-layer analyses. A vertical shear layer exists over the body surface beyond the shoulder.

Lee-surface heat-transfer results for $R_{\infty,L} = 2.4 \times 10^7$ have been plotted in Fig. 5 for different angles of attack. Heat transfer rates obtained at angles of attack did not exceed those of $\alpha = 0°$ in front of the shoulder. After the expansion over the shoulder section, however, heat transfer rates increase rapidly, indicating transition from laminar to turbulent flow. Similar results were also found for other Reynolds numbers. At relatively low angles of attack ($\alpha = 10°$, 20°), and at low Reynolds numbers, a laminar boundary layer exists over the lee surface of the nose section before the shoulder. As the Reynolds number increases, transition moves forward, resulting in higher heating (peak heating) before the flow undergoes an abrupt expansion over the shoulder section. Since there is no siginficant Reynolds number effect on the pressure field before the shoulder, the flow starts to expand at almost the same position for all Reynolds numbers whether the boundary layer is still transitional or has just become turbulent.

Maximum and secondary peak heat transfer rates obtained for various Reynolds numbers and angles of attack are shown in Fig. 6. Peak heating is plotted as a function of Reynolds number $R_{\infty,L}$. A distinction is made between the peak heating

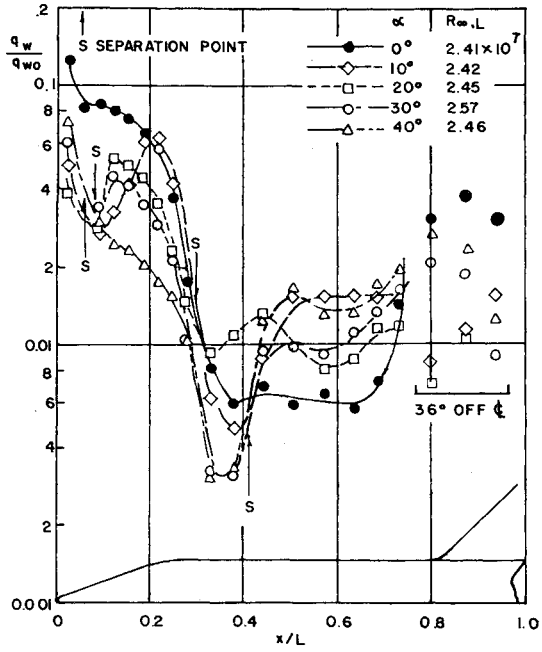

Fig. 5 Heat-transfer distributions along leeward centerline ($R_{\infty,L} \simeq 2.4 \times 10^7$.

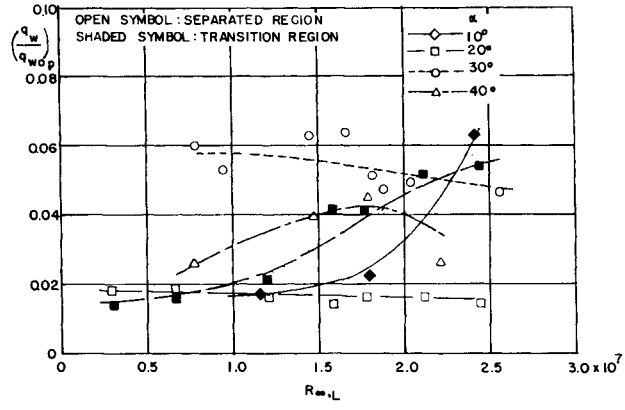

Fig. 6 Effect of Reynolds number on peak heating.

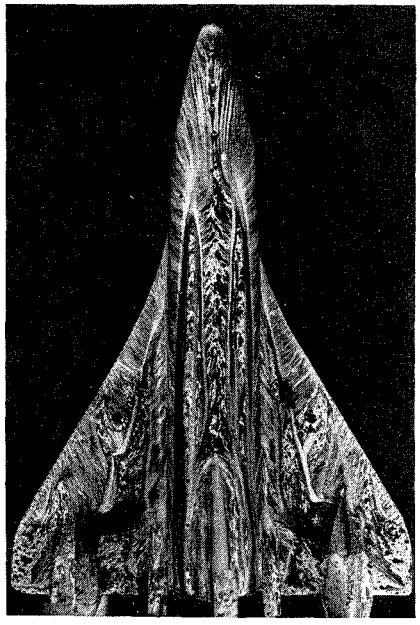

Fig. 7 Oil flow photograph of space shuttle model. ($\alpha = 20°$, $R_{\infty,L} = 2.21 \times 10^7$.

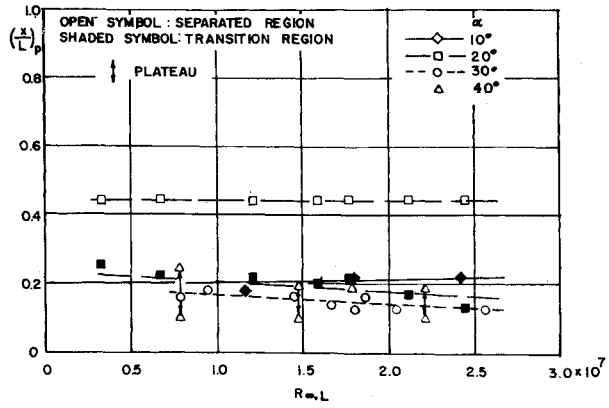

Fig. 8 Effect of Reynolds number on location of peak heating.

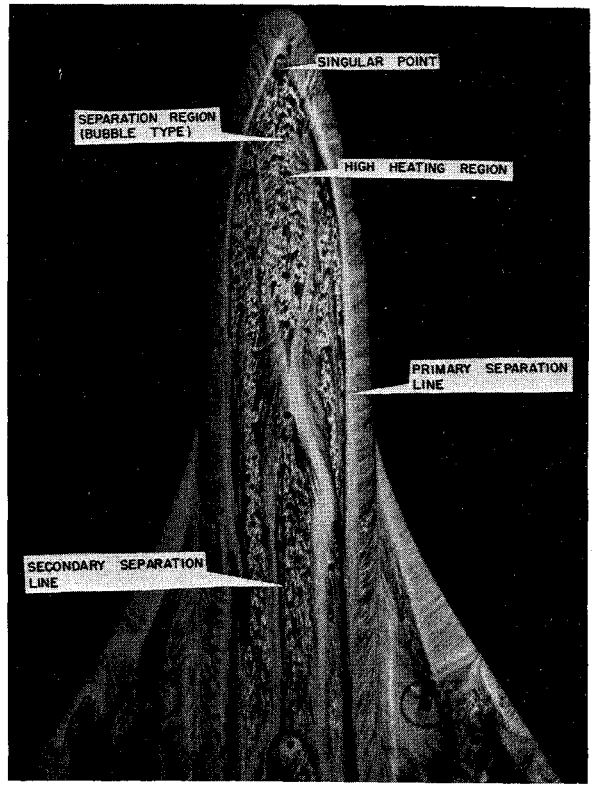

Fig. 9 Surface flow pattern near the nose of space shuttle ($\alpha = 30°$, $R_{\infty,L} = 1.43 \times 10^7$.

within a separated flow region and that due to boundary-layer transition. These results show that peak heating values due to transition are strong functions of Reynolds number and increase with $R_{\infty,L}$. Correlation of the boundary-layer transitional peak heating in terms of Reynolds number shows similar behavior as that of Ref. 8. However, peak heating within the separated region does not consistently correlate with Reynolds numbers, and seems to increase for some angles of attack and decreases for some angles of attack, as may be observed from Fig. 7.

The peak heating due to the vortex surface interaction is observed at high angles of attack ($\alpha = 20°, 30°, 40°$). As shown in Refs. 3-6, this type of peak heating is caused by the thinning of the viscous shear layer as a result of outflow induced by the vortices. The phenomenon which occurs here is conclusively not a result of the pressure distribution. This may be observed clearly from Fig. 1 for $\alpha = 30°$ and agrees with previous work.[3-6] The trend is that lower pressures are obtained as Reynolds number increases. Therefore, it can be concluded that peak heating rate within a vortex region is not caused by abrupt changes in the surface pressure distribution.

The relation between the location of peak heating and freestream Reynolds number of the present experiments is shown in Fig. 8. The location is found independently of freestream Reynolds number. Similar results have been found in Ref. 6.

Oil Flow Studies and Separation Patterns

Details of the separation lines, limiting streamlines, separated flow region, and feather-like high shear (heating) regions at various angles of attack have been given.[10] Only a summary of the oil flow studies is presented here. At relatively low angles of attack $\alpha \leq 20°$, the separation is a free vortex layer type (Fig. 7). At high angles of attack ($\alpha \geq 20°$), the separation on the front part is believed to be a bubble type (Fig. 9). In this figure, the feather-like high shear (heating) region near the leeward centerline is observed following the separated flow region immediately behind the singular point (starting point of separation). This high shear region, a kind of reattachment flow region, is created by a vortex-surface interaction, and it is here that the vortex-induced peak heating phenomenon is observed in heat transfer measurements. It is also seen that this high shear region is followed by another separated flow region corresponding to a low heat-transfer region, as confirmed by heat-transfer data.

Two pairs of separation lines were obtained for all the cases tested here with the angle of attack ranging from 10° to 40°. At $\alpha = 10°$, the inner separation line ($\varphi = 150°$) seems to be the primary line. Stetson's sharp cone result[16] is in good agreement with the inner separation line. Primary and secondary separation lines are distinguished clearly at $\alpha = 20°$. In this case the effect of Reynolds number was found to be rather significant compared to the other cases. The same pattern of separation lines (primary and secondary) is also observed at $\alpha = 30°$ and 40°. In these cases, the locations of secondary separation lines change along the body axis direction, but the primary separation lines are found to be stable over a large portion of the body from the nose part. The aforementioned results of separated flow patterns and the boundary-layer phenomena at different angles of attack suggested the possible patterns of separated flow in a cross section of the space shuttle orbiter at different ranges of angles of attack shown in Fig. 10. These patterns are deduced from the flowfield data, and the oil flow pictures are similar to those of Ref. 6.

Flowfield Surveys

Measurements of total pressure, static pressure, total temperature, and velocity profiles within the separated flow region in the leeward meridian plane have been presented.[10] Locations of the external shock determined from Schlieren photographs were also included. Large variations in both the static pressure and pitot pressure normal to the surface of the body are shown in Fig. 11 for $\alpha = 20°$. The variation of the pressure as a function of Reynolds number is quite large close to the nose region. This is due to the proximity of the measurements to the shoulder, and therefore to the location of the separated region. From the observations of the oil flow pictures for low and high Reynolds numbers, it was clearly seen that the flow patterns in this region are quite different, and therefore affect the normal pressure distribution. Further back on the body, the pressure distribution varied slightly with Reynolds number. In all measurements there seems to be a region of constant pressure normal to the body surface. This region of constant pressure could be characterized as the height of the vortex, which seems to increase with Reynolds number. Examples of total temperature and velocity profiles at $\alpha = 20°$ are given in Fig. 12. The distinct variation of the total temperature within the vortex gives an indication of the height of the vortex. The stagnation temperature is quite high even in the proximity of the surface, thus confirming the fact that there is a large inflow of high energy air towards the leeward side of the body, which gives rise to the high peak heating rates. The velocity profiles also indicate that the axial

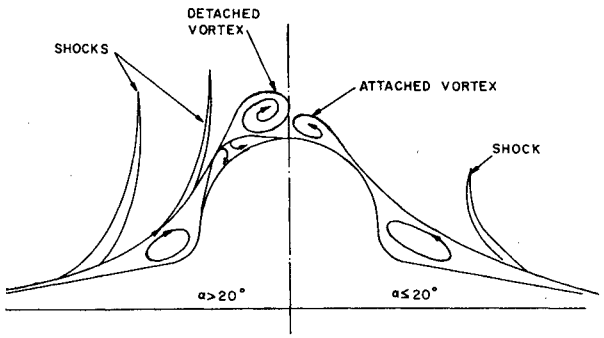

Fig. 10 Schematic of interaction for laminar and turbulent conditions.

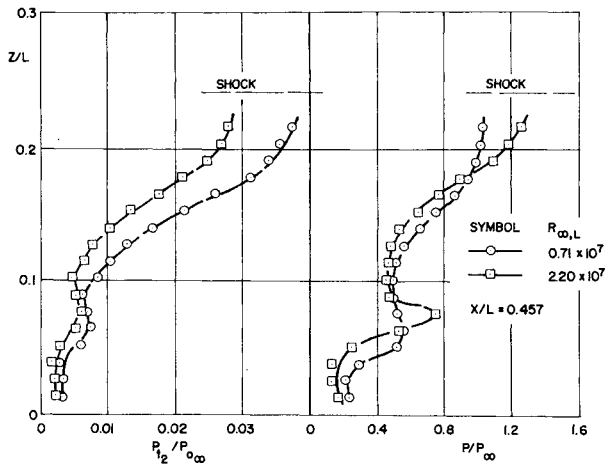

Fig. 11 Leeward centerline pressure profiles ($\alpha = 20°$).

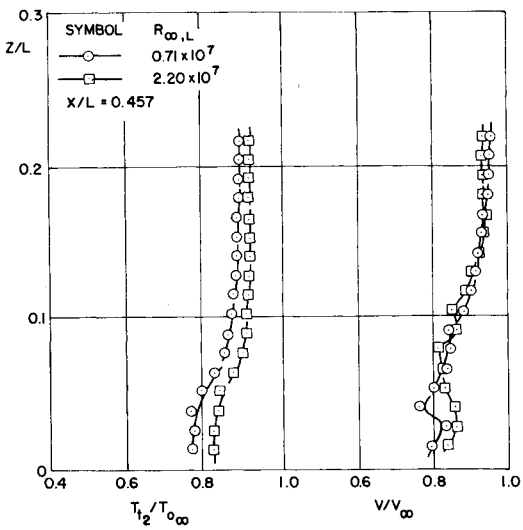

Fig. 12 Leeward centerline total temperature and velocity profiles ($\alpha = 20°$).

velocity within the vortex region is quite large and must not be considered as a dead air region, as usually is indicated within a separated region.

The present total pressure measurements are also plotted in the form of $C_{p,\text{pitot}}$. When plotted in this manner the present results agree very well with the results of Ref. 17 and show little variation as a function of the normal distance from the body. Profiles of static pressure have not been measured in Ref. 17 and no conclusions could be made for the type of velocity that can be obtained within the vortex region. Therefore, it is concluded here that,in order to deduce the velocity distribution within the vortex, stagnation temperature, static pressure, and total pressure measurements have to be obtained.

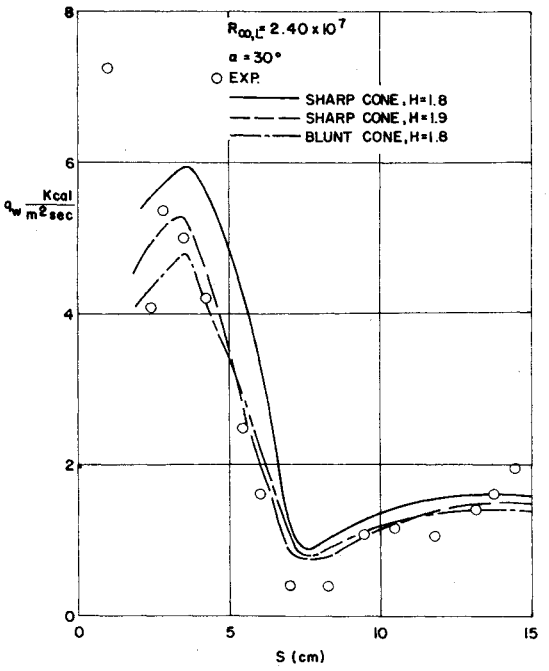

Fig. 13 Comparison of leeward centerline heat-transfer rates between turbulent boundary-layer theory and experiments ($\alpha = 30°$).

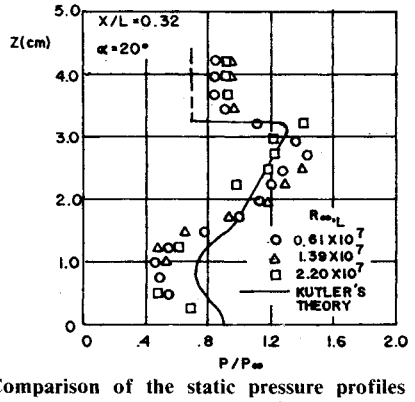

Fig. 14 Comparison of the static pressure profiles between experiments and inviscid flow theory ($\alpha = 20°$).

IV. Theoretical Analysis of the Leeward Centerline Heat Transfer

In the previous results and discussion sections, attached boundary-layer theory has been used to estimate approximately the leeward centerline heat transfer rates. The effect of flow separation at various angles of attack has not been considered. In this section, results of an existing turbulent boundary-layer theory, taking into account the separation, is presented. The momentum integral equation of compressible turbulent boundary layer is solved numerically. The expression of local skin friction in terms of reference properties and boundary-layer shape factor[14] is used. Local heat-transfer rates are calculated from the Reynolds analogy.

Assumptions

The theory and numerical method for solving a turbulent compressible boundary layer with pressure gradients and cross flow have been developed by Zakkay et al.[18] This method is used to predict the present leeward surface centerline heat transfer measurements. The following assumptions were made: a) The boundary-layer shape factor is $1.8 \approx 1.9$. b) An axisymmetric body, with local radius the same as the distance from the leeward centerline of the model to its body axis was used. c) The effects of cross flow and normal pressure gradient are neglected. d) Two extreme stagnation pressures were used to determine the local external flow conditions. The local inviscid stagnation pressure was assumed constant at the values behind either the normal shock or the conical shock due to a cone of 19.3° half angle in Mach 5.93 freestream.

Comparisons between Theory and Experiments

Only the experimental results with the largest freestream Reynolds number of 2.40×10^7 are considered. At an angle of attack, present numerical results agree with measurements, especially for the cases of large angle of attack, $\alpha = 30°$ (Fig. 13). This also indicates that transition of laminar to turbulent occurs when the model is at small angle of attack ($\alpha = 10°$).

The relation between the boundary-layer thickness and the shape factor for turbulent boundary layer with pressure gradient has been found by Truckenbrodt.[19] The boundary layer separated at $H = 1.8 \sim 1.9$. These values were used in the present computation to account for the separation. The variation of the shape factor, as a function of the local momentum thickness, has not been considered. An initial momentum thickness must be given to carry out the numerical integration step by step and it was estimated by the method of Ref. 14 for the present studies. Further improvement of the numerical results can be made if detailed circumferential pressure measurements are available to estimate the cross-flow effect.

V. Analysis of Flowfield

Results of the present experimental investigation and the discussions of the flowfield measurements over yawed cone[10] provide some necessary ingredients to analyze the flowfield over the space shuttle and the interaction between the flowfield and the vortices. The method proposed here is a semi-empirical procedure which utilizes an equivalent body shape to develop the flowfield. The equivalent body is derived from a combination of viscous turbulent boundary layer up to the point of separation, and a correlation of flowfield data within the separated region. From the equivalent body, the flowfield is calculated using an inviscid program modified to analyze the flow over the complicated geometry.

Physical Model

The physical model incorporated the concept of an "effective" body to represent the region of high shear layer, including both the boundary layer and the vortices. It was considered to be enclosed by a streamline or stream surface, which divided the region of high shear from the outer inviscid shock layer. Once the effective body shape was determined, Kutler's method[20] for analyzing the flowfield over 3-dimensional configurations at high angle of attack can be used to determine the inviscid flowfield over the effective body surface.

To characterize the effective body shape in the separated region and to define the surface conditions, a boundary-layer computation scheme is required. The boundary-layer theory, including the streamline tracing concept with small cross-flow assumptions, can be utilized for this purpose because it provides the 3-dimensional capability which is an essential feature of the viscous flow phenomena in this study.

Determination of the Effective Body Shape

The effective body will be established by an iteration procedure wherein different body shapes are prescribed as input to a computer program until a satisfactory match of the calculated surface pressure with measurements is obtained. As had been indicated in studies of the oil flow and separation patterns, the separation pattern over the space shuttle configuration is similar to that over the yawed cone. Thus, correlation of the surface pressure measurements over yawed cones[21] can be used to generalize the nominal body shape.

Numerical Example

To evaluate the previous procedure in determining the flowfield, a simplified analysis was performed for the present space shuttle configuration. An axially symmetric body was chosen having the body profiles of leeward plane of symmetry of the model. An equivalent body was constructed over the space shuttle model at $\alpha = 20°$. The numerical pressure distribution on the leeward plane of symmetry, obtained from Kutler's method, is compared with the results of profile measurements in Fig. 14. Comparisons indicate that: a) The inviscid flow theory over the equivalent body predicts the experimental pressure profile satisfactorily for $\alpha = 20°$, and larger surface pressure was obtained from the theory. b) Locations of the external shock obtained from the numerical method and experiment are also in good agreement. The complicated geometry of the space shuttle model has not been properly considered in the present studies. However, considering the assumptions made for this analysis, it is rewarding to see that results of the proposed method show the trends of experimental measurements.

VI. Conclusions

Investigations of heat-transfer and flow separation phenomena over a space shuttle model at large angles of attack have been performed. The main efforts have been directed toward the understanding of the leeward side flow phenomena associated with flow separation. Experiments have been conducted at Mach 6, with high Reynolds numbers $1.64 - 13.1 \times 10^7$/m and large angles of attack. From the present studies, the following conclusions have been reached:

1) There is a large Reynolds number effect on the pressure distribution on the leeward side of the space shuttle. A lower pressure level exists for an increasing Reynolds number. The largest variation is observed to exist at 30° angle of attack.

2) At small angles of attack (10°, 20°), the boundary layer on the nose varies from laminar to transitional, then to turbulent, as the Reynolds number increases. The separation of a free-vortex-layer type occurs after the shoulder on the leeward side. At larger angles of attack (30°, 40°) , bubble-type separation, starting at a singular point, exists near the nose region and is immediately followed by a feather-like high heating region. This high heating region is reattachment region created by vortex-surface interaction.

3) There are two distinct types of high heating rates on the lee surface of a space shuttle configuration: peak heating due to boundary-layer transition and peak heating associated with vortex interactions within a separated flow region. The former appeared at relatively low angles of attack (10°, 20°), and the latter was observed at relatively large angles of attack (20°, 30°, 40°). At 20° angle of attack both types of heating peaks appeared.

4) The peak heating due to boundary-layer transition correlated with the freestream Reynolds number; the heating value increases rapidly with the Reynolds number. The maximum peak heating due to vortex-surface interactions (vortex-induced peak heating) occurs for an angle of attack of 30°.

5) Large axial component of velocity is calculated in the separated flow region over the space shuttle leeward surface. These results were obtained from measurements of static pressure, total pressure, and stagnation temperature. It is indicated here that pitot pressure measurements alone are not sufficient to deduce velocity profiles, since large static pressure and temperature gradients exist normal to the surface.

6) At large angle of attack turbulent boundary-layer theory, with a shape factor of 1.8-1.9, predicts the heat-transfer rates satisfactory, especially for the case with high Reynolds number.

7) The effect of vortex interaction on the pressure field of the space shuttle can be evaluated by an inviscid analysis performed over an appropriate fictitious "equivalent body" surface, which accounts for viscous effects. Preliminary analysis of this type of model for analyzing the flowfield seems to agree with the flowfield measurements.

References

[1] Whitehead, A.H., Jr. and Keys, J.W., "Flow Phenomena and Separation over Delta Wings with Tailing-Edge Flaps at Mach 6," *AIAA Journal,* Vol. 6, Dec. 1968, pp. 2380-2387.

[2] Whitehead, A.H., Jr., "Effect of Vortices on Delta Wing Lee-Side Heating at Mach 6," *AIAA Journal,* Vol. 8, March 1970, pp. 599-600.

[3] Whitehead, A.H., Jr., Hefner, J.N., and Rao, D.M., "Lee Surface Vortex Effects over Configurations in Hypersonic Flow," AIAA Paper 72-77, San Diego, Calif, 1972.

[4] Hefner, J.N. and Whitehead, A.H., Jr., "Lee-Side Heating Investigations, Part I-Experimental Lee-Side Heating Studies on a Delta-Wing Orbiter," *NASA Space Shuttle Technology Conference,* Vol. I, TM X-2272, Dec. 1971, pp. 267-287, NASA.

[5] Hefner, J.N. and Whitehead, A.H., Jr., "Lee-Side Flow Phenomena on Space Shuttle Configurations at Hypersonic Speeds, Part II-Studies of Lee-Surface Heating at Hypersonic Mach Numbers," *Space Shuttle Aero-Thermodynamics Technology Conference,* Vol II, TM X-2507, Feb. 1972, pp. 451-467, NASA.

[6] Hefner, J.N., "Lee-Surface Heating and Flow Phenomena on Space Shuttle Orbiters at Large Angles of Attack and Hypersonic Speeds," TN D-7088, 1972, NASA.

[7] Wang, K.C., "Separation Patterns of Boundary Layer over an Inclined Body of Revolution," *AIAA Journal,* Vol. 10, Aug. 1972, pp. 1044-1050.

[8] Maskell, E.C., "Flow Separation in Three Dimensions," Report Aero. 2565, 1955, Royal Aeronautical Establishment, England.

[9] Lees, L., "Laminar Heat Transfer over Blunt-Nosed Bodies at Hypersonic Flight Speeds," *Jet Propulsion,* Vol. 26, April 1956, pp. 259-269.

[10] Zakkay, V., Miyazawa, M., and Wang, C.R., "Lee-Surface Flow Phenomena over Space-Shuttle at Large Angles of Attack at $M_\infty = 6$," New York University, N.Y., 1974.

[11] Sims, J.L., "Tables for Supersonic Flow around Right Circular Cones at Zero Angle of Attack," SP-3004, 1964, NASA.

[12] Tracy, R.R., "Hypersonic Flow over a Yawed Circular Cone," GALCIT Hypersonic Research Project Memorandum, 69, 1963.

[13] Eckert, E.R.G. and Tewfik, O.E., "Use of Reference Enthalpy in Specifying the Laminar Heat-Transfer Distribution around Blunt Bodies in Dissociated Air," *Journal of the Aero/Space Sciences,* Vol. 27, June 1960, pp. 464-466.

[14] Reshotko, E. and Tucker, M., "Approximate Calculation of the Compressible Turbulent Boundary Layer with Heat-Transfer and Arbitrary Pressure Gradient," TN-4154, 1957, NACA.

[15] Eckert, E.R.G., "Engineering Relations for Friction and Heat Transfer to Surfaces in High Velocity Flow," *Journal of the Aeronautical Sciences,* Vol. 22, Aug. 1955, pp. 585-587.

[16] Stetson, K.F., "Boundary-Layer Separation on Slender Cones at Angle of Attack," *AIAA Journal,* Vol. 10, May 1972, pp. 642-648.

[17] Cleary, J.W., "Lee-Side Flow Phenomena on Space Shuttle Configuration at Hypersonic Speeds," TM X-2507, Feb. 1972, NASA.

[18] Zakkay, V., Calarese, W., and Wang, C.R., "Hypersonic Turbulent Boundary Layer with Pressure Gradients and Cross Flow," *AIAA Journal,* Vol. 10, Nov. 1972, pp. 1393-1394.

[19] Schlichting, H., "Boundary-Layer Theory," 4th ed., McGraw-Hill, N.Y., pp. 570-571, 1960.

[20] Kutler, P., Warming, R.F., and Lomax, H., "Computation of Space Shuttle Flowfields Using Noncentered Finite Diference Schemes," *AIAA Journal,* Vol. 11, Feb. 1943, pp. 196-204.

[21] Zakkay, V., Economos, C., and Alzner, E., "Lee-side Flow Field Description over Cones at Large Incidence," AFFDL-TR-94-19, Air Force Flight Dynamics Lab., Wright-Patterson Air Force Base, Ohio.